Simulation of Pressure Buildup in a Multiphase Wellbore/Reservoir System

P.H. Winterfeld, Marathon Oil Co.

Summary. A pressure-buildup test is simulated in a system consisting of a wellbore and a reservoir and containing multiphase fluid. Wellbore flow is governed by conservation of matter and momentum, and reservoir flow by conservation of matter and Darcy's law. Finite-difference versions of the flow equations are solved on a discretized system. A single-phase example illustrates wellbore storage and wellbore fluid inertia shortly after shut-in. Two-phase examples illustrate phase redistribution, and one shows a "hump" caused by phases segregating. Buildup and other data from a field case are also matched.

Introduction

A pressure-buildup test consists of shutting in a producing reservoir. The bottomhole pressure (BHP) response in such a test is determined by factors in both the reservoir (such as boundaries, heterogeneities, and fractures) and the wellbore. The theoretical description of reservoir factors is detailed and well documented.[1] However, such is not the case for wellbore factors.

For the most part, the effect of the wellbore on a pressure-buildup test has been described in terms of two phenomena: wellbore storage and phase redistribution. Wellbore storage, noted by van Everdingen and Hurst,[2] has been described in detail by Ramey.[3] When a producing reservoir is shut in at the surface, fluid continues to flow from the reservoir into the wellbore (afterflow) for a time because the wellbore contents are compressible. In addition, if the wellbore contents are multiphase, there will be phase redistribution. Redistribution of a relatively incompressible, heavier liquid phase flowing simultaneously with a relatively compressible, lighter vaporous phase causes the wellbore to pressurize. This may be relieved by flow of wellbore fluid back into the reservoir (backflow) and can be manifested as a "hump" on a Horner plot of BHP response.[4] Another factor besides wellbore storage and phase redistribution that affects pressure buildup is wellbore fluid inertia.[5] In addition, wellbore fluid can exchange heat with the surroundings, but this is beyond the scope of this paper.

The effect of wellbore storage on BHP has been described by use of a wellbore storage coefficient[3]:

$$qB+C_{wbs}(dp_{bh}/dt)=0. \quad \ldots\ldots (1)$$

Eq. 1 is a mass balance. The first term is influx and the second is accumulation of mass in the wellbore. Fair[6] modified Eq. 1 to describe phase redistribution as well by adding a phase-redistribution pressure (p_{pr}) to p_{bh}, where

$$p_{pr}=C_{pr}(1-e^{-\Delta t_{ws}/\alpha_{pr}}). \quad \ldots\ldots (2)$$

C_{pr} and α_{pr} are parameters used to match field data. Eqs. 1 and 2 are empirical relationships that describe with good accuracy the gross BHP response following shut-in. However, the details of wellbore flow are not described by these equations. For instance, fluid properties vary significantly over the wellbore length, which can be several miles, and wellbore fluid is often multiphase. The wellbore storage coefficient in Eq. 1 is an average over the length and phases of the wellbore. The functional form of p_{pr} in Eq. 2 was chosen because it mimics laboratory data; no physical justification was given for it. A rigorous treatment of wellbore flow during pressure buildup is needed to facilitate interpretation of field data. Such a treatment is the subject of this paper.

Governing Equations

Multiphase flow in the wellbore is governed by conservation of matter—

$$\frac{\partial}{\partial t}(y\rho)_k+\frac{\partial}{\partial z}(y\rho u)_k=-\sum_{\ell\neq k}\dot{m}_{k,\ell}, \quad \ldots\ldots (3)$$

where $\dot{m}_{k,\ell}$=rate of mass transfer from Phase k to Phase ℓ per unit volume—and conservation of momentum[7]—

$$\frac{\partial}{\partial t}(y\rho u)_k+g_c y_k\frac{\partial p}{\partial z}=g_c(y\gamma)_k-\sum_{\ell\neq k}\dot{m}_{k,\ell}u_k+\sum_{\ell\neq k}F_{k,\ell}+F_{k,w}, \quad \ldots\ldots (4)$$

where $F_{k,\ell}$=viscous force between Phases k and ℓ per unit volume and $F_{k,w}$=viscous force between Phase k and the wellbore per unit volume. Eq. 4 is a momentum balance over a thin cross section of wellbore. Normal shear and momentum transport from convection have been neglected and uniform phase pressure is assumed. Phase/phase continuity conditions for conservation of mass and momentum are,[7] respectively,

$$\dot{m}_{k,\ell}=-\dot{m}_{\ell,k} \quad \ldots\ldots (5)$$

and $$\dot{m}_{k,\ell}u_k-F_{k,\ell}=-\dot{m}_{\ell,k}u_\ell+F_{\ell,k}. \quad \ldots\ldots (6)$$

Multiphase flow in the reservoir, a porous medium, is governed by conservation of matter and Darcy's law.[8]

Flow Formulation

Fluid flow is simulated in a system consisting of a cylindrical reservoir with a wellbore centered at the origin. Up to three phases may be present (the formulation is applicable to any number of phases): vaporous and liquid hydrocarbon phases and water. Hydrocarbons consist of two conserved species: gas and stock-tank oil. Hydrocarbon thermodynamics allows both species to be present in a phase, with gas primarily composing the vaporous phase and stock-tank oil primarily composing the liquid phase. Hydrocarbon is not soluble in water, which is also a conserved species.

A pressure-buildup test consists of two intervals: production and shut-in. During production, fluid flows from the reservoir, into and up the wellbore, and out at the surface. A pseudosteady-state approximation is applied to flow in the wellbore because wellbore volume is small compared with the volume of fluid moving through it during production and because properties of fluid flowing from the reservoir into the wellbore change slowly with time. A consequence of pseudosteady state is that wellbore pressure, and phase holdup and velocity profiles, are independent of past history. To simulate events after shut-in, the wellbore profiles need only be computed at the instant of shut-in. During production, the simulation is a conventional reservoir one. At the instant of shut-in, the wellbore profiles are computed from (1) Eq. 3 at steady state,

$$\frac{\partial}{\partial z}(y\rho u)_k=-\sum_{\ell\neq k}\dot{m}_{k,\ell}, \quad \ldots\ldots (7)$$

(2) Eq. 4 at steady state summed over all phases,

$$g_c(\partial p/\partial z)=\sum_k g_c(y\gamma)_k+F_{k,w} \quad \ldots\ldots (8)$$

(Eq. 6 eliminates the terms $F_{k,\ell}$ and $\dot{m}_{k,\ell}u_k$), and (3) a multiphase-flow correlation. Correlations have been developed[9,10] that predict pressure and phase holdup profiles along the wellbore from the properties of the material entering and Eqs. 7 and 8. In addition, the

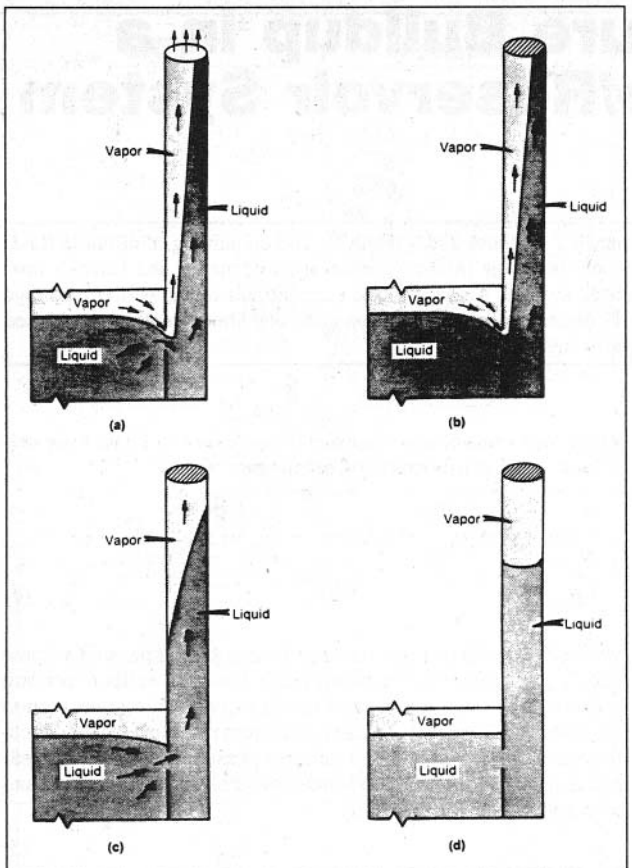

Fig. 1—Schematic of wellbore/reservoir system showing (a) production, (b) the instant of shut-in, (c) an intermediate time during shut-in, and (d) static equilibrium.

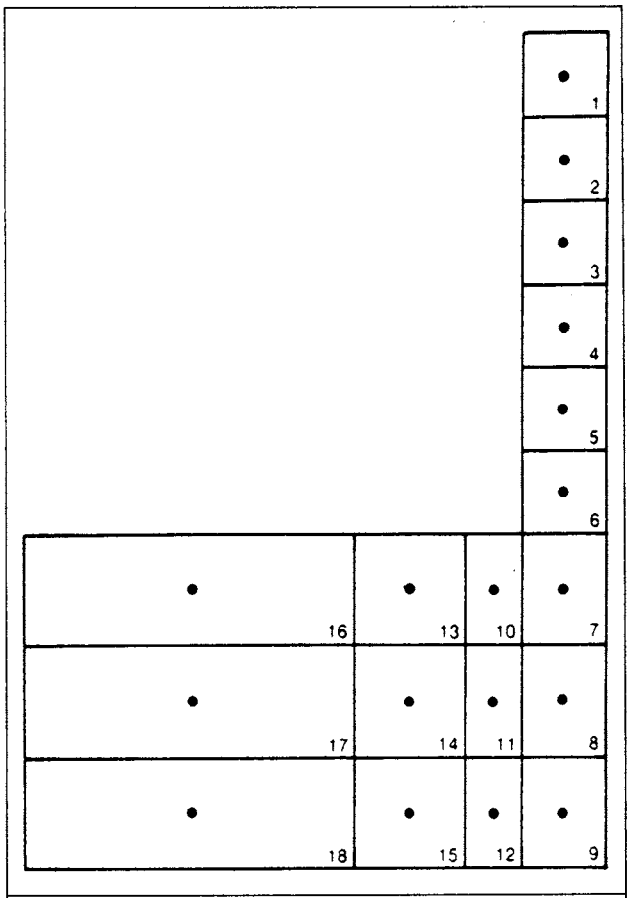

Fig. 2—Schematic of discretized wellbore/reservoir system. Gridblock number appears in lower right corner.

correlations predict the flow regime; i.e., the form or geometry of flow. These correlations were obtained from laboratory experiments and are empirical.

At shut-in, the top of the wellbore is closed off. Then, the system approaches static equilibrium, with phase segregation in the wellbore, exchange of material between it and the reservoir, and fluid motion eventually ceasing. Figs. 1a through 1d show flow during a pressure-buildup test in a wellbore/reservoir system.

Semiempirical expressions are derived for the viscous-force terms. For single-phase flow, the phase/wellbore term is

$$F_{k,w}(y_k=1)=58.0582\{[(F_f N_{\mathrm{Re}}\mu u)_k]/(2r_w^2)\}, \quad \ldots\ldots\ldots\ldots (9)$$

where friction factor, F_f, and Reynold's number, N_{Re}, are related through the Colebrook function:

$$1/\sqrt{F_f}=-4\ \log\left[(\epsilon/89.28\ r_w)+\left(1.255/N_{\mathrm{Re}}\sqrt{F_f}\right)\right]. \quad \ldots\ldots (10)$$

In multiphase flow, Eq. 9 is reduced by a function of phase holdup. Phase/wellbore viscous force is often small compared with other forces (e.g., gravity) operating during multiphase flow in a vertical wellbore. Therefore, a linear function is assumed:

$$F_{k,w}=58.0582\{[(F_f N_{\mathrm{Re}}\mu u y)_k]/(2r_w^2)\}. \quad \ldots\ldots\ldots\ldots\ldots (11)$$

When two phases are in relative motion, a drag force is exerted between them. Phase/phase viscous force is correlated as the product of the drag coefficient, C_D; interfacial area, A; and relative velocity, u_r, squared:

$$F_{k,\ell}\equiv C_D A u_r^2. \quad \ldots\ldots\ldots\ldots\ldots\ldots\ldots\ldots\ldots (12)$$

For many cases of laminar flow, such as gas bubbles rising in liquid (Stokes' law) or stratified two-phase flow between a pair of flat plates, the drag coefficient is inversely proportional to relative velocity (Reynolds' number). As flow becomes turbulent, the drag coefficient often tends to be less sensitive to changes in relative velocity.[11] Dependence of phase/phase viscous force on relative velocity is assumed to vary between linear and quadratic. Interfacial area is dependent on phase holdup. As phase holdup vanishes, interfacial area does also, and the ratio of phase surface to volume becomes infinite (this can be illustrated by imagining the phase as dispersed spherical droplets whose radii shrink to zero). A simple functional representation of interfacial area for Phases k and ℓ is

$$A_{k,\ell}\approx(y^\omega)_k(y^\omega)_\ell,\ 0<\omega_k,\omega_\ell<1. \quad \ldots\ldots\ldots\ldots\ldots\ldots (13)$$

The exponent ω must be greater than zero to ensure vanishing interfacial area as holdup vanishes. Phase volume is proportional to phase holdup, so ω must be less than one to ensure infinite surface/volume ratio as holdup vanishes. The phase/phase viscous-force term for Phases k and ℓ is thus

$$F_{k,\ell}=C_{k,\ell}(y^\omega)_k(y^\omega)_\ell(u_k-u_\ell)|u_k-u_\ell|^{\omega_u},0<\omega_k,\ \omega_\ell,\omega_u<1. \quad \ldots\ldots\ldots\ldots\ldots\ldots\ldots\ldots\ldots\ldots (14)$$

Coefficients $C_{k,\ell}$ are solved for by substituting Eq. 14 into Eq. 4 at steady state with all terms evaluated at the instant of shut-in:

$$\sum_{\ell\neq k} C_{k,\ell}G_{k,\ell}=\left[g_c y_k\frac{\partial p}{\partial z}-g_c(y\gamma)_k+\sum_{\ell\neq k}\dot{m}_{k,\ell}u_k-F_{k,w}\right]\Bigg|_{\Delta t_{ws}=0}, \quad \ldots\ldots\ldots\ldots\ldots\ldots\ldots\ldots (15)$$

where $G_{k,\ell}\equiv(y^\omega)_k(y^\omega)_\ell(u_k-u_\ell)|u_k-u_\ell|^{\omega_u}|_{\Delta t_{ws}=0}$. $\ldots\ldots (16)$

For n phases, Eq. 15 yields $n-1$ algebraic equations for $C_{k,\ell}$; the number of $C_{k,\ell}$ is the binomial coefficient $\binom{n}{2}$. $C_{k,\ell}$ is uniquely determined for a two-phase system and there is one degree of freedom for a three-phase system. In the case of vaporous and liquid-hydrocarbon phases and water, the vaporous/liquid hydrocarbon and vaporous-hydrocarbon/water coefficients can be set equal.

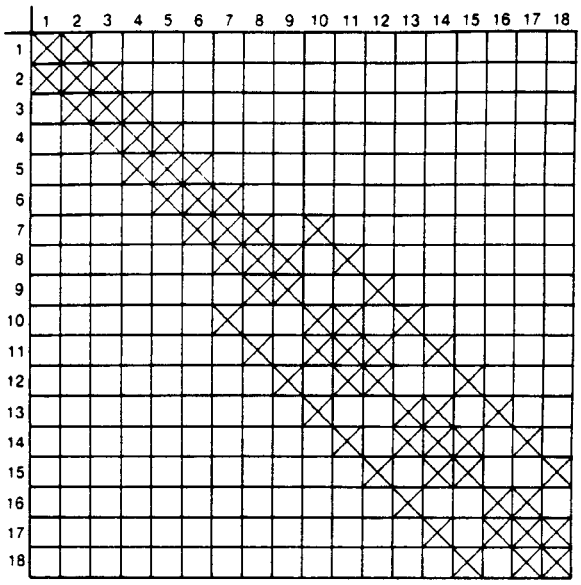

Fig. 3—Incidence matrix for grid in Fig. 2.

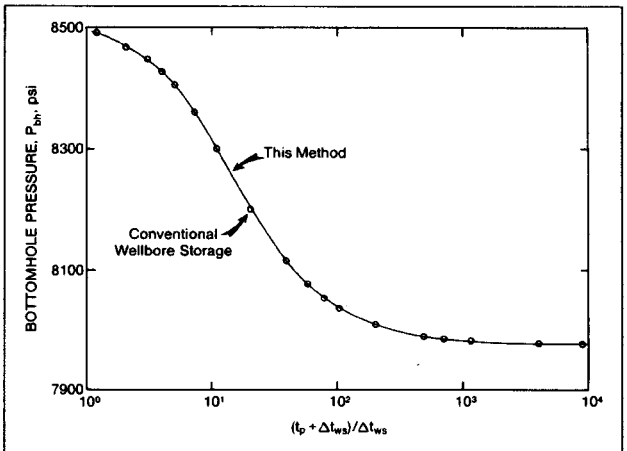

Fig. 4—Horner plot for single-phase buildup.

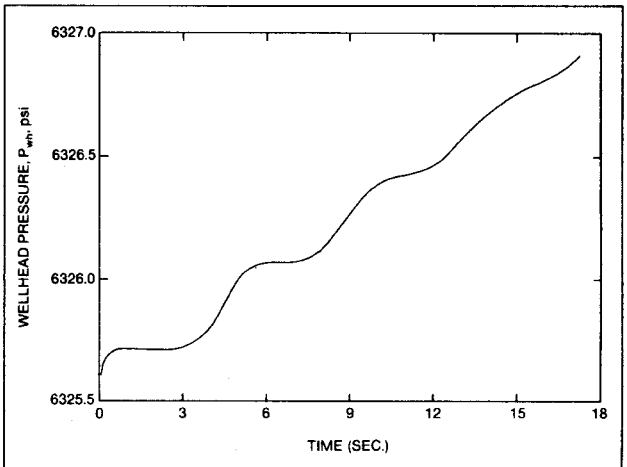

Fig. 5—Wellhead pressure vs. time for single-phase buildup.

Flow Solution

The equations governing flow in the wellbore/reservoir system (Eqs. 3 and 4) are solved with a fully implicit finite-difference approximation. Fig. 2 shows an example of a finite-difference grid. Reservoir flow is restricted to two-dimensional r-z coordinates and wellbore flow is axial. Reservoir layers that are perforated exchange fluid with the wellbore. The reservoir and wellbore are strongly coupled; flow of fluid between the reservoir and wellbore is proportional to the pressure difference there. Details of the finite-difference approximations for the wellbore appear in the Appendix.

The nonlinear flow equations are solved by Newton iteration. Fig. 3 is the incidence matrix for the grid in Fig. 2. Inversion of the matrix occurs by first upper triangulating the portion corresponding to wellbore gridblocks above the reservoir (numbered 1 through 6 in Fig. 2). Reservoir gridblocks and wellbore gridblocks adjacent to the reservoir are no longer coupled to wellbore gridblocks above the reservoir. These gridblocks form a rectangular array and are solved next by D-4 Gaussian elimination. Solution for wellbore gridblocks above the reservoir then proceeds by back-substitution.

Results and Discussion

Single-Phase Example. A pressure-buildup test was simulated with a single-phase, slightly compressible fluid. The system was produced at a constant rate and then shut in. The Horner plot, Fig. 4, illustrates wellbore storage. Flow from the reservoir into the wellbore continues after the well is shut in because fluid in the wellbore is compressible. Influx of mass into the wellbore causes BHP to increase, thereby decreasing the rate of afterflow. Thus, the Horner plot approaches the semilog straight line that the reservoir, shut in at the sandface, would show. Fig. 4 also includes the Horner plot obtained with Eq. 1 to describe wellbore storage. The wellbore storage coefficient was calculated from wellbore volume and an average of fluid properties between the wellhead and reservoir.[1] Identical Horner plots from these two methods are expected for this single-phase case. Eq. 1 neglects the effects of fluid flow in the wellbore; i.e., friction and inertia. These effects are small, however, and have negligible influence on the Horner plot.

Fig. 5 is a plot of simulated wellhead (top wellbore gridblock) pressure vs. time just after shut-in. At shut-in, the top of the wellbore is abruptly closed. The inertia of fluid flowing up the wellbore causes a pressure oscillation that damps out because of friction between the fluid and the wellbore. The oscillation is superposed on an approximately linear buildup caused by afterflow. During

TABLE 1—WELLBORE PROFILES FOR FIRST TWO-PHASE BUILDUP AT SHUT-IN

Layer	Pressure (psi)	Holdup (fraction)		Velocity (ft/D)	
		Vapor	Liquid	Vapor	Liquid
1	4,703	0.0924	0.9076	82,490	9,730
3	4,968	0.0844	0.9156	82,563	9,962
5	5,233	0.0773	0.9227	83,170	10,225
7	5,498	0.0702	0.9298	84,015	10,485
9	5,761	0.0628	0.9372	84,808	10,772
11	6,025	0.0558	0.9442	85,450	11,046
13	6,289	0.0489	0.9511	86,889	11,332
15	6,553	0.0417	0.9583	88,985	11,662
17	6,817	0.0341	0.9659	91,785	12,021
19	7,081	0.0262	0.9738	88,541	12,403
21	7,282	0.0241	0.9759	0	0

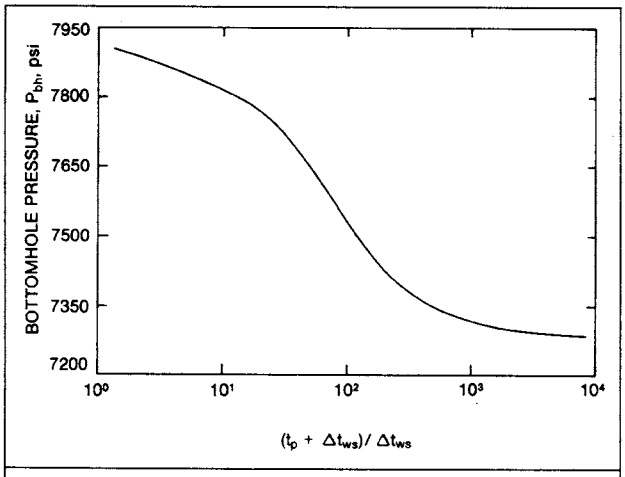

Fig. 6—Horner plot for first two-phase buildup.

the time between pressure peaks, the pressure oscillation travels down and up the wellbore (twice the wellbore length). The resulting oscillation speed agrees with the theoretical value of a pressure pulse (sound) in a slightly compressible fluid. Simulation of pressure buildup in an effectively single-phase wellbore has been reported elsewhere; e.g., in geothermal applications.[12]

Two-Phase Examples. Pressure-buildup tests with two phases, vaporous and liquid hydrocarbon (black oil), were also simulated. Hydrocarbon fluid in the wellbore, as well as in the reservoir, was assumed to be in vaporous/liquid equilibrium that is governed by input solubility functions of pressure (i.e., solution GOR for liquid phase and gas/liquid content for vapor phase). The wellbore was discretized into 21 layers. Pressure and phase holdup and velocity profiles in the wellbore at shut-in calculated with the Hagedorn and Brown[10] two-phase flow correlation are shown in Table 1. Vaporous-phase velocity is greater than liquid-phase velocity and liquid holdup increases toward the bottom of the wellbore, a result of liquid-phase slippage. The lighter vaporous phase must "drag" the heavier liquid phase up the wellbore. Fig. 6 is the Horner plot of the BHP buildup. Although it is similar to the single-phase one (Fig. 4), wellbore flow during buildup in the two-phase case differs markedly from the single-phase case. In addition to afterflow, which occurs in both, phases redistribute in the two-phase case, with vaporous and liquid phases completely segregated after a sufficiently long time. Phase segregation causes the wellbore to pressurize, and sufficiently large pressurization will cause the Horner plot to have a hump. Table 2 shows wellbore profiles at shut-in, and Fig. 7 is the Horner plot for another two-phase buildup, produced under conditions different from the previous plot. In this one, a hump occurs around an abscissa value of 100. The hump contains a local maximum of BHP. Backflow must occur for a time after the pressure maximum, at least until BHP starts increasing. Backflow is not always sufficient to cause decreasing BHP, however. BHP changes are caused by two factors: exchange of mass between the wellbore and reservoir and wellbore pressurization resulting from phase segregation. If the pressurization component is large enough, BHP can still increase if backflow is not too large. Table 3 shows vaporous holdup profiles at various times after shut-in. Vaporous holdup toward the top of the wellbore tends to increase with time, and that toward the bottom of the wellbore tends to decrease with time, eventually resulting in segregated phases at static equilibrium. Shortly after shut-in, however, vaporous holdup around the middle of the wellbore (Layers 3 through 5) first decreases somewhat and then increases. Decrease in vaporous holdup occurs because, shortly after shut-in, the wellbore is pressurizing greatly, causing vapor to dissolve in the liquid.

Values of ω used above for vaporous and liquid hydrocarbon phases and velocity, respectively, were 0.75, 0.25, and 0.0. Variation of ω caused a slight displacement of the Horner plot with essentially no change in shape.

Field Case. The wellbore/reservoir simulator was applied to a field case. Data matched were layer flow rates and BHP during production and the buildup after shut-in. The reservoir grid was four layers with 10 radial subdivisions. Drainage and wellbore radius, layer thickness, elevation, and porosity, fluid and rock properties, and production schedule were given. Layer permeability, skin factor, and initial pressure were match parameters. The reservoir initially contained unsaturated liquid hydrocarbon. Table 4 shows field data during production, and Table 5 shows the match by simulation. Wellhead pressures are not included in Table 5 because wellbore pressure is calculated only at the instant of shut-in. Table 6 shows wellbore profiles at shut-in. The bubblepoint pressure of liquid hydrocarbon is crossed at a point in the wellbore; hence, wellbore flow is single-phase below that point and two-phase above. Differences between BHP and wellhead pressure in Table 4 are typically 3,300 to 3,400 psi [22.8 to 23.4 MPa]. The pressure profile in Table 6 shows a similar difference. A two-phase flow correlation can be inaccurate if applied to conditions different from those under which it was constructed. A grossly inaccurate holdup profile at shut-in will not result in a realistic pressure-buildup simulation, especially for the times when wellbore effects dominate the Horner plot. One way to ascertain whether the holdup profile is reasonably accurate is to measure simultaneously BHP and wellhead pressure, preferably at the instant of shut-in. These measured pressures can be compared with calculated values, and if there is disagreement, parameters involved in the correlation can be adjusted or another correlation can be used. Fig. 8 is the match of field data with simulation for the buildup. The influence of the wellbore ends around an abscissa value of 300. Field data are then linear to an abscissa value of 10, then deviate upward. This behavior has been matched with a composite reservoir; permeability and porosity far from the wellbore were lower than they were near the wellbore. The actual cause of the upward deviation need not be a composite reservoir; such a deviation could be caused by a fault as well.

The simulation was repeated with conventional wellbore storage (Eq. 1) substituted for the discretized wellbore. The result also appears in Fig. 8. Wellbore storage coefficient was calculated from a log-log data plot[1] by use of the data point at Horner time 1,201. Simulation does not match field data, indicating that wellbore effects are much more complex than just wellbore storage.

Conclusions

A new technique has been developed for simulating pressure buildup in a wellbore/reservoir system. This technique is much more sophisticated than previous ones, which handled flow in a gross manner. The formulation of wellbore flow is rigorous, based on conservation of mass and momentum, and has yielded fruitful results both in understanding flow in a wellbore/reservoir system and in interpreting buildup data from the field.

TABLE 2—WELLBORE PROFILES FOR SECOND TWO-PHASE BUILDUP AT SHUT-IN

Layer	Pressure (psi)	Holdup (fraction)		Velocity (ft/D)	
		Vapor	Liquid	Vapor	Liquid
1	1,742	0.7211	0.2789	9.52×10^5	4.80×10^5
3	2,109	0.6682	0.3318	8.16×10^5	4.31×10^5
5	2,528	0.6158	0.3842	7.23×10^5	3.99×10^5
7	2,992	0.5548	0.4452	6.60×10^5	3.66×10^5
9	3,506	0.4778	0.5222	5.34×10^5	3.94×10^5
11	3,934	0.4898	0.5102	0	0

Nomenclature

A = interfacial area, ft^2 [m^2]
B = FVF, RB/STB [res m^3/stock-tank m^3]
C = drag coefficient, various units
C_D = drag coefficient, lbm/ft^6 [kg/m^6]
C_{pr} = phase redistribution parameter, psi [kPa]
C_{wbs} = wellbore storage coefficients, RB/psi [res m^3/kPa]
F = viscous force per unit volume, lbm/ft^2-D^2 [kg/$m^2 \cdot d^2$]
F_f = Fanning friction factor
g_c = conversion factor in Newton's second law of motion, 3.4586×10^{13} lbm/psi-ft-D^2
$\dot{m}$ = phase/phase mass-transfer rate per unit volume, lbm/ft^3-D [kg/$m^3 \cdot d$]
N_{Re} = Reynold's number
p = pressure, psi [kPa]
p_{bh} = bottomhole pressure, psi [kPa]
p_{pr} = phase redistribution pressure, psi [kPa]
p_{wh} = wellhead pressure, psi [kPa]
q = wellbore/reservoir flow rate, STB/D [stock-tank m^3/d]
r_w = wellbore radius, ft [m]
t = time, days
t_p = production time, days
Δt = timestep size, days
Δt_{ws} = shut-in time, days
u = velocity, ft/D [m/d]
u_r = relative velocity, ft/D [m/d]
V = gridblock volume, ft^3 [m^3]
y = holdup
z = wellbore elevation, ft [m]
α_{pr} = phase redistribution parameter, days
γ = phase gradient, psi/ft [kPa/m]
ϵ = pipe roughness, in. [cm]
μ = viscosity, cp [Pa·s]
ρ = density, lbm/ft^3 [kg/m^3]
ϕ = porosity
ω = exponent parameter

Subscripts

k,ℓ = phase
m = gridblock number
n = timestep number
u = velocity
w = wellbore

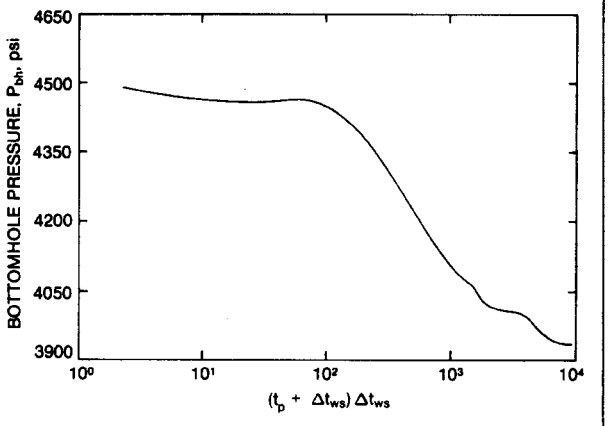

Fig. 7—Horner plot for second two-phase buildup.

Acknowledgment

I thank Marathon Oil Co. for permission to publish this paper.

References

1. Earlougher, R.C. Jr.: *Advances in Well Test Analysis*, Monograph Series, SPE, Richardson, TX (1977) **5.**
2. van Everdingen, A.F. and Hurst, W.: "Application of the Laplace Transform to Flow Problems in Reservoirs," *Trans.*, AIME (1949) **186,** 305-24.
3. Ramey, H.J. Jr.: "Non-Darcy Flow and Wellbore Storage Effects in Pressure Build-Up and Drawdown of Gas Wells," *JPT* (Feb. 1965) 223-33; *Trans.*, AIME, **234.**
4. Kazemi, H. *et al.*: "Complexities of the Analysis of Surface Shut-In Drillstem Tests in an Offshore Volatile Oil Reservoir," *JPT* (Jan. 1983) 173-77.
5. Stegemeier, G.L. and Matthews, C.S.: "Study of Anomalous Pressure Build-Up Behavior," *Trans.*, AIME (1958) **213,** 44-50.
6. Fair, W.B. Jr.: "Pressure Buildup Analysis With Wellbore Phase Redistribution," *SPEJ* (April 1981) 259-70.
7. Banerjee, S. and Chan, A.M.C.: "Separated Flow Models—I," *Intl. J. Multiphase Flow* (1980) **6,** 1-24.
8. Shank, G.D. and Vestal, C.R.: "Practical Techniques in Two-Pseudocomponent Black-Oil Simulation," *SPERE* (May 1989) 244-52.
9. Orkiszewski, J.: "Predicting Two-Phase Pressure Drops in Vertical Pipe," *JPT* (June 1967) 829-38; *Trans.*, AIME, **240.**
10. Hagedorn, A.R. and Brown, K.E.: "Experimental Study of Pressure Gradients Occurring During Continuous Two-Phase Flow in Small-Diameter Conduits," *JPT* (April 1965) 475-84; *Trans.*, AIME, **234.**

TABLE 3—VARIOUS HOLDUP PROFILES AT VARIOUS TIMES AFTER SHUT-IN FOR SECOND TWO-PHASE BUILDUP

		Vaporous Holdup (fraction)				
Layer	Shut-In	6.5 Minutes	11.0 Minutes	30.7 Minutes	50.8 Minutes	138.5 Minutes
1	0.7211	0.8878	0.9347	0.9815	0.9904	0.9975
3	0.6682	0.6293	0.6864	0.9123	0.9587	0.9906
5	0.6158	0.5490	0.5317	0.6804	0.9033	0.9908
7	0.5548	0.4590	0.4251	0.2581	0.0707	0.0000
9	0.4778	0.3518	0.2960	0.1193	0.0370	0.0009
11	0.4898	0.2588	0.0868	0.0000	0.0000	0.0000

TABLE 4—LAYER LIQUID RATE AND PRESSURE DATA DURING PRODUCTION

Time	Layer Liquid Rate (STB/D)				p_{bh}	p_{wh}
(days)	1	2	3	4	(psi)	(psi)
96.1	8,641	10,506	1,993	0	4,530	1,246
96.4	6,969	6,136	907	0	4,858	1,524
96.7	5,422	3,128	332	0	5,050	1,669

TABLE 5—SIMULATED LAYER LIQUID RATES AND BOTTOMHOLE PRESSURE

Time	Layer Liquid Rate* (STB/D)				p_{bh}
(days)	1	2	3	4	(psi)
96.1	10,033 (16%)	9,134 (13%)	1,973 (1%)	0	4,628 (2%)
96.4	7,122 (2%)	5,863 (4%)	1,027 (13%)	0	4,890 (1%)
96.7	5,032 (7%)	3,500 (12%)	350 (9%)	0	5,089 (1%)

*Percentages in parentheses are differences between simulation and field data.

TABLE 6—WELLBORE PROFILES FOR FIELD CASE AT SHUT-IN

Layer	Pressure (psi)	Holdup (fraction)		Velocity (ft/D)	
		Vapor	Liquid	Vapor	Liquid
1	1,018	0.7020	0.2980	2.87×10^{6}	2.33×10^{6}
3	1,246	0.6362	0.3638	2.43×10^{6}	1.95×10^{6}
5	1,503	0.5540	0.4460	2.20×10^{6}	1.61×10^{6}
7	1,797	0.4415	0.5585	2.00×10^{6}	1.42×10^{6}
9	2,126	0.3499	0.6501	1.89×10^{6}	1.29×10^{6}
11	2,483	0.2629	0.7371	1.87×10^{6}	1.21×10^{6}
13	2,866	0.1663	0.8337	2.16×10^{6}	1.14×10^{6}
15	3,278	0.0472	0.9528	0	1.11×10^{6}
17	3,714	0	1.0000	0	1.16×10^{6}
19	4,148	0	1.0000	0	1.15×10^{6}
21	4,483	0	1.0000	0	0.34×10^{6}
23	4,559	0	1.0000	0	0

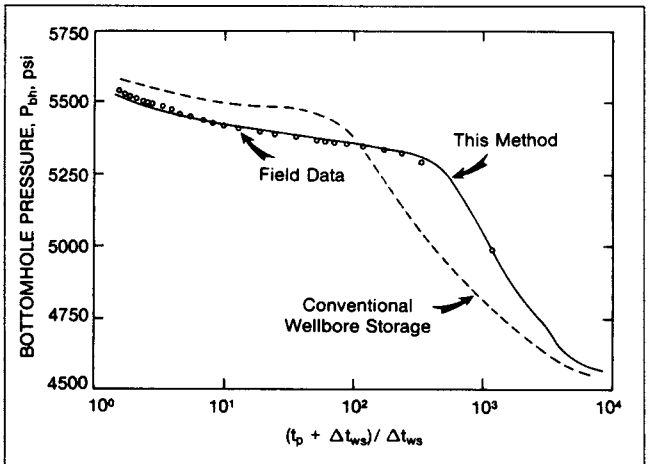

Fig. 8—Horner plot showing match of field case from this method and the result with conventional wellbore storage.

11. Perry, J.H.: *Chemical Engineers' Handbook*, McGraw-Hill Book Co., New York City (1963).
12. Miller, C.W.: "Numerical Model of Transient Two-Phase Flow in a Wellbore," report LBL-9056, U.S. DOE (Oct. 1979).

Appendix—Finite-Difference Approximation for Wellbore Flow Equations

Fully implicit, finite-difference approximations of Eqs. 3 and 5 are solved in the wellbore. For Gridblock m with volume V at time interval $n+1$, the approximation for Eq. 3 is

$$(V/\Delta t)[(y\rho)_m^{n+1}-(y\rho)_m^n]+\Sigma(\pi r_w^2 y\rho u)_{m\pm\frac{1}{2}}^{n+1}=-\dot{m}|_m^{n+1}, \quad \ldots(A\text{-}1)$$

where the subscripts k and ℓ are understood and the subscripts $m\pm\frac{1}{2}$ refer to gridblock interfaces. At gridblock interfaces, phase holdup and density are evaluated "upstream" and phase velocity is evaluated next.

The approximation for Eq. 5 uses a control volume spanning the interval between two adjacent gridblock nodes:

$$y^{n+1}[(\rho u)^{n+1}-(\rho u)^n]/\Delta t+g_c(\nabla p)^{n+1}-g_c(\gamma)^{n+1}+(\dot{m}u)^{n+1}$$
$$-F_w^{n+1}=F^{n+1}. \quad \ldots(A\text{-}2)$$

Phase/wellbore viscous force and momentum transfer caused by phase/phase mass flux are included on the left side of Eq. A-2 because they are proportional to phase holdup and can be included with the other such terms in parentheses. Phase/phase viscous force is not proportional to phase holdup and appears on the right side of Eq. A-2. Pressure gradient is evaluated by use of pressure at the gridblock nodes spanning the control volume, and phase holdup is the geometric mean of phase holdup at those nodes. Other representations of phase holdup, such as the arithmetic mean, gave unsatisfactory results. Eq. A-2 depends on phase velocity at a single gridblock interface and thus eliminates phase velocity from Eq. A-1.

The hollow wellbore is orders of magnitude more permeable than the porous reservoir. As a result, the precision of at least a 48-bit computer is needed to solve the coupled set of wellbore and reservoir flow equations. Very small timesteps are also required. Timestep size is typically 0.25 second just after shut-in and is gradually increased as the rate of wellbore pressurization begins to subside.

SI Metric Conversion Factors

bbl	× 1.589 873	E−01	= m^3
ft	× 3.048*	E−01	= m
psi	× 6.894 757	E+00	= kPa

*Conversion factor is exact.

SPEFE

Original SPE manuscript received for review Oct. 5, 1986. Paper accepted for publication Oct. 5, 1987. Revised manuscript received May 9, 1988. Paper (SPE 15534) first presented at the 1986 SPE Annual Technical Conference and Exhibition held in New Orleans, Oct. 5–8.